



encit 2020



18<sup>th</sup> Brazilian Congress of Thermal Sciences and Engineering  
November 16-20, 2020 (Online)

## ENC-2020-0630

### STUDY OF PRECIPITATION OF CaCO<sub>3</sub> CRYSTALS BY PHOTOMICROSCOPY

**Rafael de Paula Cosmo**

**Rodrigo Simoes Maciel**

**Romulo Fieni Fejoli**

Postgraduate Program in Mechanical Engineering, Federal University of Espirito Santo, Vitoria, ES, Brazil  
rpcosmo@gmail.com; rodrigossimoesrsm@gmail.com; romulofieni@hotmail.com

**Fabio de Assis Ressel Pereira**

Department of Industrial Technology, Federal University of Espirito Santo, Vitoria, ES, Brazil  
f.ressel@gmail.com

**Edson Jose Soares**

Department of Mechanical Engineering, Federal University of Espirito Santo, Vitoria, ES, Brazil  
edson.soares@ufes.br

**Daniel da Cunha Ribeiro**

Department of Engineering and Technology, Federal University of Espirito Santo, Sao Mateus, ES, Brazil  
daniel.ribeiro@ufes.br

**Andre Leibsohn Martins**

**Marcus Vinicius Duarte Ferreira**

Petrobras, Rio de Janeiro, RJ, Brazil  
aleibsohn@petrobras.com.br, mvdferreira@petrobras.com.br

**Abstract.** *Inorganic salts fouling is one of the operational problems that pose major challenges to flow assurance of oil and gas exploration and production. In order to act effectively in the mitigation of this phenomenon, it is important to understand its behavior under the conditions in which they occur, whether in the porous medium and / or in the completion equipment. Photomicroscopy technique can be an effective tool to achieve this goal as it has the ability to provide measurement of the equivalent diameter of a particle – even if it is under to high pressures and temperatures. The aim is to compare photomicroscopy to a consolidated technology for determining particle or drop size distribution (PSD or DSD). The procedure consists of the dispersion of solid calcium carbonate (CaCO<sub>3</sub>) in water and simultaneous analysis by photomicroscopy and laser diffraction. Comparison of the PSD diagrams of the two techniques validates the procedure for ambient pressure and temperature. The next step is to perform this procedure on a pressurized and heated reactor.*

**Keywords:** CaCO<sub>3</sub>, crystals, photomicroscopy, PSD, laser diffraction

#### 1. INTRODUCTION AND JUSTIFICATION

Inorganic scaling is a problem that spends a large amount of time, money and human resources in the oil industry (Zhang, Allan and Hugh, 2015). Scaling anywhere in production system is only the final step of a process that begins when ions dissolved in the brine undergo conditions also favorable to the nucleation of solid crystals (Cosmo et al., 2019). Growth of such crystals and agglomeration are intermediate steps of this process.

These phenomena are represented in Figure 1 for calcium carbonate salt forming. The sketch is a simplified view of an extremely complex flow, in which the oily and gaseous phases have been suppressed to allow an easier understanding of the phenomena of interest.

To effectively mitigate and remedy this phenomenon, it is essential to investigate the temperature and pressure conditions under which they occur. For example: a suspension of barium sulphate (BaSO<sub>4</sub>), given by Eq. (1), is 67% smaller at 100 °C and 100 atm (actual well conditions) than at 25 °C and 1 atm (ambient conditions of current laboratory analysis) (Crabtree et al., 1999).



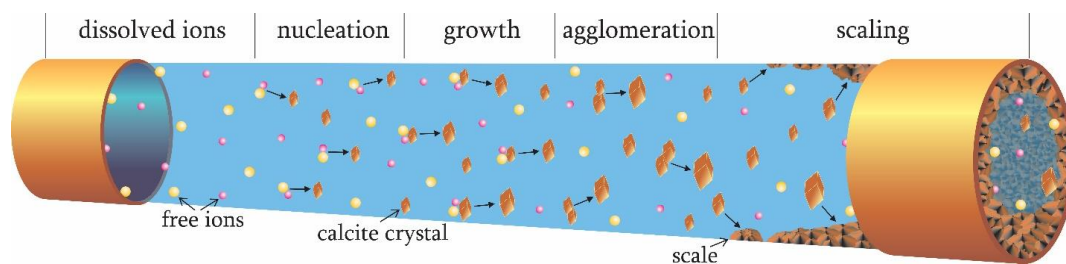


Figure 1. Main phenomena involved in inorganic scaling, in this case, calcite scaling.  
 Available from: Cosmo et al. (2019).

The concentration of salts in the produced water can vary from 10 to 400 g/L, affecting the ionic strength and, consequently, the solubility of the minerals. Under certain pressure and temperature conditions, the solubility of strontium sulphate (SrSO<sub>4</sub>) is about 7 times higher at 180 mg/L than near zero concentrations (Crabtree et al., 1999).

For carbonate salts such as calcium carbonate (CaCO<sub>3</sub>), discrepancies that are even more serious may occur. Carbon dioxide (CO<sub>2</sub>) dissolves in water, changing the concentrations of carbonate species. The analytical distribution of inorganic carbon between species as a function of pH (Fig. 2) is directly affected by pressure and temperature.

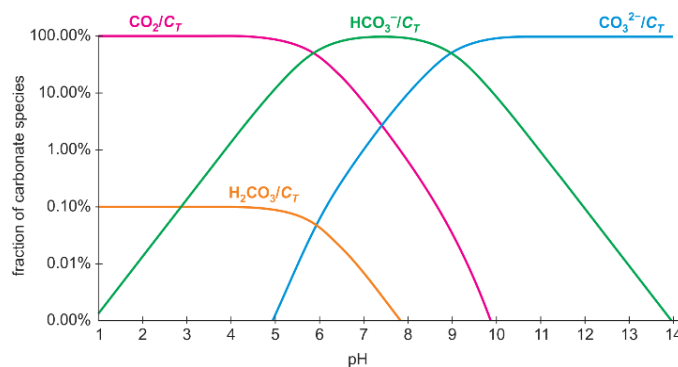


Figure 2. Analytical distribution of inorganic carbon as a function of pH (CT = Total Carbonate).  
 Available from: Waly (2011) [adapted].

As shown by Cosmo et al. (2019), the effects of CO<sub>2</sub> released from water (degassing, outgassing, exsolution, or flash effect) due to the pressure drop caused by oil production is much more pronounced than the thermodynamics of salt solubility, given by Eq. (2).



Eq. (2) is valid for pressurized systems in the presence of CO<sub>2</sub>, which is very common in carbonate reservoirs such as pre-salt oil province, in Brazil. Under these conditions, pressure solubilizes CO<sub>2</sub> in water, acidifying the aqueous medium. When the system depressurizes, bicarbonate (HCO<sub>3</sub><sup>-</sup>) available in solution reacts with calcium, precipitating CaCO<sub>3</sub> and releasing CO<sub>2</sub>.

In common laboratory tests, atmospheric pressure is not sufficient to significantly solubilize CO<sub>2</sub>. The aqueous medium is more basic, favoring the predominance of carbonate (CO<sub>3</sub><sup>2-</sup>). Thus, the reaction governing the phenomenon is as follows:



Polymorphism is another issue that may influence the analysis. Calcium carbonate, for example, may occur in the form of three crystalline phases (anhydrous phases): calcite, aragonite and vaterite – all as CaCO<sub>3</sub> (Fig. 3); or as three hydrated phases: amorphous calcium carbonate, monohydrocalcite (CaCO<sub>3</sub>·H<sub>2</sub>O) and hexahydrocalcite (CaCO<sub>3</sub>·6H<sub>2</sub>O).

The hydrated phases of calcium carbonate are metastable, called “precursors” because they quickly turn into the more stable anhydrous phases (Brečević & Nielsen, 1989). At ordinary temperatures in petroleum environments, aragonite would only stabilize at a pH around 11 (Tai & Chen, 1998), which is not expected from the reservoir to surface facilities, whose pH is usually in the range of 4 to 8. At ambient pressure and temperature, vaterite is the preferred form, especially when saturating the solution with CO<sub>3</sub><sup>2-</sup> or HCO<sub>3</sub><sup>-</sup>, raising pH and making vaterite the only form present (Kogo, Umegaki and Kojima, 2019).

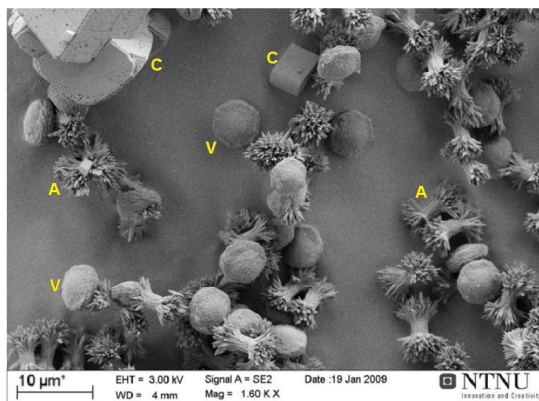


Figure 3. Calcite (C) coexisting with vaterite (V) and aragonite (A) under laboratory conditions.  
Available from: Beck and Andreassen (2010).

In the case of calcite, for a petroleum environment where high temperatures are observed, if the system is highly supersaturated a transition phase is expected, while for low supersaturation the direct formation of calcite is more common. Calcite is the most frequently found polymorph, as it has the greatest stability under the conditions of operations derived from petroleum activity (Cowan and Weintritt, 1976; Eseosa and Atubokiki, 2011).

The presence of other ions should also be considered. Besides affecting the solubility of the species, it alters the size and shape of the crystals (Fig. 4), and consequently the dynamics of precipitation and scale adhesion.

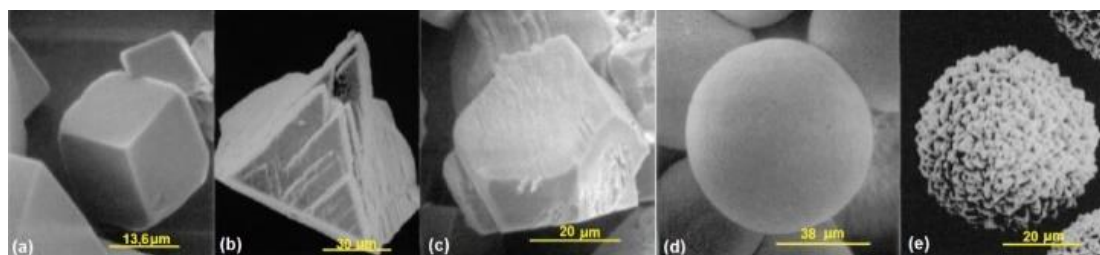


Figure 4. Calcite: (a) pure; (b) with  $Mg^{2+}$ ; (c) with  $SO_4^{2-}$ ; (d) with  $Mg^{2+}$  and  $SO_4^{2-}$ ; (e) with less  $Mg^{2+}$  and  $SO_4^{2-}$ .  
Available from: Tracy, François and Jennings (1998).

In summary: Assessing inorganic salt formation under conditions that do not simulate oil environments can lead to very discrepant errors, leading to economically disastrous operational and design decisions. In order to allow close-to-real investigations, it is proposed to use a pressurized reactor with thick borosilicate viewing windows. Many experiments can be performed with this equipment, especially those to investigate the phenomena shown in Figure 1. However, it is first necessary to validate the measurement techniques of the parameters to be evaluated.

In this paper, we are validating a noninvasive technique for measuring particle size distribution. It will be very important when performing pressurized and heated experiments.

## 2. PHOTOMICROSCOPY

The photomicroscopy technique consists of coupling a high-resolution camera to a microscope capable of enlarging a sample and capture a digital image (Brown, 2009). The illumination is a key point to capture quality images. The main ways are: reflection; direct or diffuse transfection; and transmission. The most common are reflection (the light beam and the microscope are placed in front of the sample) and transmission (the sample lies between the light beam and the microscope). The disposal of the transfection is similar to that of reflection, but needs to place a mirror behind the sample.

Once the images are obtained, their content can be evaluated by simple visual inspection, aiming to identify morphologies, interaction between elements, spatial distribution, among many other features (Ingham, 2012). However, it is common to use a software developed to measure some characteristics, such as the area of each particle or drop, its dimensions, the distance between adjacent particles or drops, among others. Data can be exported to a spreadsheet and worked, or the software itself may be able to post-process, thereby generating useful information (Pepper, Gerba & Gentry, 2015).

Situations in which the material analyzed is spherical are uncommon. Thus, one can determine the equivalent diameter of each particle or drop, which is the diameter of the circumference of the same area (Brown, 2009).

Equivalent diameters can be grouped into predefined bands, giving the absolute and relative amounts of the particles or drops belonging to each band, and thus generating a particle or drop size distribution diagram (PSD or DSD).

Another feature of great interest to the technique is the non-interference in the process, since it is noninvasive. Thus, it is possible to evaluate pressurized, heated, cooled, acidic, or toxic systems, which in many cases is inaccessible to other techniques. Figure 5 shows a cryostat-coupled photomicroscopy system which operates at temperatures below – 250 °C (cryogenic temperatures) (Russell, Cleary and Reeves, 2012).

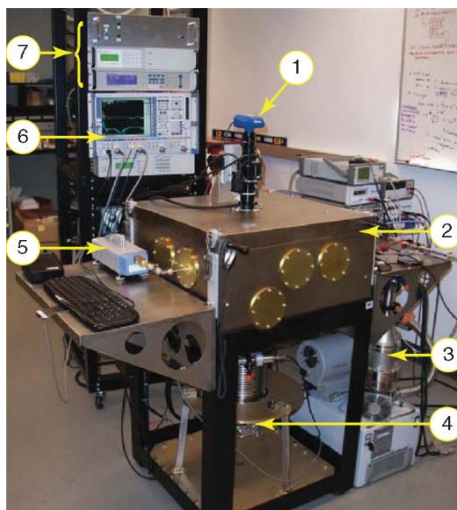


Figure 5. Photomicroscopy system (#1) coupled to a cryostat (#2) for cryogenic temperature analysis.  
Available from: Russell, Cleary and Reeves (2012).

### 3. LASER DIFFRACTION

Laser diffraction technique consists in the detection of diffracted photons due to the incidence of a laser beam on particles or drops in a translucent liquid. It is one of the most established techniques for determining particle size (Horiba, 2009; Horiba, 2017) and is applicable to particle sizes ranging from approximately 0.1  $\mu\text{m}$  to 3 mm (ISO 2009).

Light interacts in four different ways with an obstacle: reflection; refraction; diffraction and absorption (Horiba, 2009). Depending on the size and shape of the obstacles, light diffracts (or scatters) differently (Fig. 6). The smaller the particle or droplet, the greater the dispersion angle (Horiba, 2017).

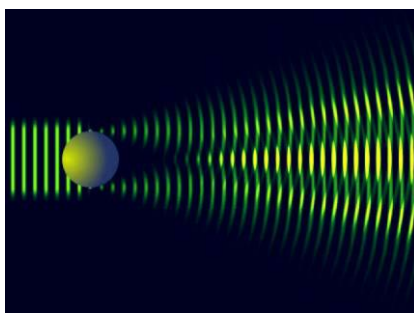


Figure 6. Idealized edge diffraction of a flat wave incident on a spherical particle.  
Available from: Horiba (2009).

As the detectable content enters or leaves the illuminated area, the diffraction pattern changes as it depicts the instantaneous distribution of particles or drops. A set of detectors captures the diffraction patterns, and a computer analyzes the data to infer the particle or droplet sizes at that moment (Horiba, 2017; Hennock, Rahalkar and Richmond, 1984).

The optical model of analysis is important. The pioneer, the Fraunhofer Approach (Joseph von Fraunhofer), is inaccurate for sizes smaller than 20 microns (Horiba, 2009). Mie scattering theory (Gustav Mie) is an analytical solution, not an approximation, with precision (Fig. 7) even in nanometer dimensions (Malvern, 2007a; Horiba, 2017). Once the particles or droplets have been measured, it is possible to generate a PSD or DSD diagram, as in the photomicroscopy technique.

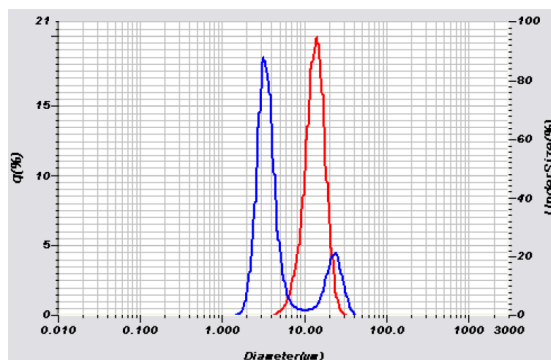


Figure 7. Glass beads of known diameter correctly “measured” by Mie (red) and wrongly by Fraunhofer (blue). Available from: Horiba (2017).

## 4. METHODOLOGY

One way to validate the photomicroscopy technique by the laser diffraction technique is to compare the respective PSDs diagrams generated from aliquots of the same saline solution. For this aim, both techniques were performed at laboratory pressure and temperature conditions (1 atm and 23 °C), and the saline solution have been formed by powdered calcium carbonate ( $\text{CaCO}_3$ ) dispersed in distilled water. The entire procedure was performed with the expectation of guaranteeing the same analysis conditions for both techniques.

### 4.1 Materials and Equipment

Calcium carbonate used has the following description: 99.04% content; molecular weight 100.09; appearance of white fine powder. The main features of the photomicroscopy equipment are (Fig. 8): Ring LED Light A5351FA036 Techniquip; Dual Bifurcated Gooseneck LED Light Guides MISDPL24+ Techniquip; Mitutoyo 10X 34 mm objective lens; UltraZoom 6000@ lens Navitar, Inc.; short adapter 3.3X Navitar, Inc.; PAXcam5+™ 5 MP digital camera PAX-it™.

With this apparatus, it is possible to capture particles of equivalent diameter from 1 micron in a solution. It depends on the level of magnification that can get well-focused images, which is limited by the type of material, concentration, agitation and other factors. Captured images were post-processed and analyzed with PAX-it™ Image Analysis (MIS, 2019). The data was exported to a spreadsheet to generate PSD diagrams.

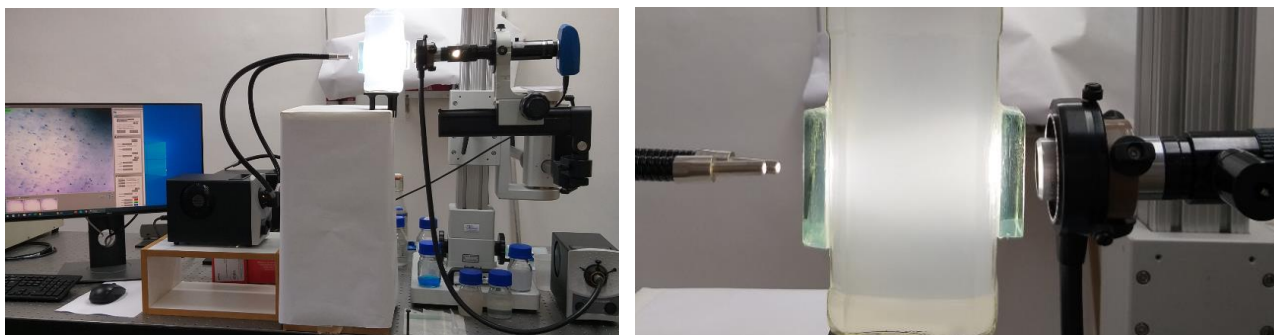


Figure 8. Equipment used for photomicroscopy imaging and lighting details.

The application of laser diffraction technique was carried out with Mastersizer 2000E equipment (Malvern, 2007a) and with Hydro 2000MU sample dispersion unit (Malvern, 2007b), both by ©Malvern Instruments Ltd. This set is capable of performing wet sample analysis and detecting particles in the range of 0.1 to 1000 µm. Upon completion of the measurement, the optical bank raw data were analyzed by the Mastersizer Software, which include several information, like PSD diagram, percentile D(0.1), D(0.5) and D(0.9), uniformity, span, and others.

### 4.2 Procedures

The very fine calcium carbonate powder was dispersed in distilled water to form a 0.080 g/L concentration solution. After a brief manual stirring, the analyzes were performed. With the photomicroscopy equipment already calibrated, some snapshots of the crystals present in the solution were obtained. Several images were stored for post-processing

and analysis. Images were taken with both illumination features: by dual bifurcated gooseneck LED light guides; by ring LED light; and both at the same time (Fig. 8).

In diffraction equipment, some precautions had to be taken to ensure almost the same analysis conditions as the photomicroscopy technique. The ultrasonic probe, which aids in sample dispersion and removes bubbles, has not been used. At first, the stirrer would not be used in either technique as the impeller and vessel geometries would provide very different shear rates. If the analyzes yielded different results, new runs would be performed with the least possible stirring. Three measurements were completed and the raw data stored for further analysis and post processing.

Image analysis and post-processing were performed with PAX-it!<sup>TM</sup> Software. However, they were exported to a spreadsheet software to generate the PSD diagrams with the same scales and shapes reported by Mastersizer software. In PAX-cam Software, some filters and other imaging features have been applied to produce a better analyzable image. Some zones with differences in lighting intensity were observed, so only the brightest part of the images was analyzed.

In Mastersizer Software, Mie scattering theory needs some inputs to work. Water was selected from software database as the dispersant with refractive index equal to 1.33. For the “Material”, calcium carbonate was selected with refractive index equal to 1.69 and absorption equal to 0.1, considering the red laser beam wavelength of 633 nm.

## 5. RESULTS AND DISCUSSIONS

### 5.1 Photomicroscopy Analysis

In photomicroscopy experiments, illumination by the transmission technique (dual bifurcated gooseneck LED light guides – Fig. 9 left, brought better results than the reflection technique (ring LED light – Fig. 9 middle). With both techniques at the same time, no gain was observed compared to the transmission technique alone. Ten best focused images were selected for analysis. With the PAX-it!<sup>TM</sup> Software, the equivalent particle diameter ( $\phi$ ) of each image was determined. All data were exported to a spreadsheet and some statistical parameters were calculated (Table 1). To avoid errors in particle area detection, Figure 9 left was cut. This image has been analyzed (PSD in Fig. 9 right) to provide the results for Run 3 in Table 1.

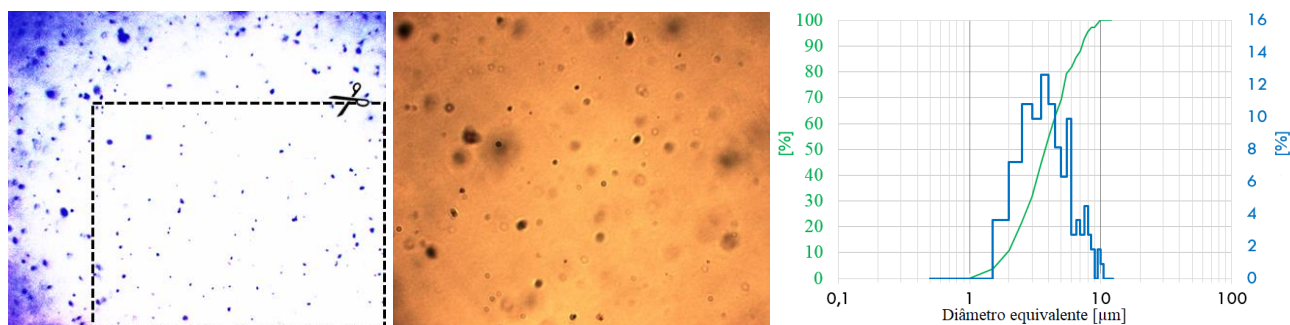


Figure 9. Image obtained with transmission technique (left); image obtained with reflection technique (middle); PSD diagram for the cut area of the image in the left, equivalent for ‘Run 3’ (right).

Table 1. Statistical parameters calculated for data from ten selected images for the photomicroscopy analysis.

Run	Mean $\phi$ ( $\mu\text{m}$ )	Median $\phi$ ( $\mu\text{m}$ )	Range $\phi$ ( $\mu\text{m}$ )	Mode $\phi$ ( $\mu\text{m}$ )	Largest $\phi$ ( $\mu\text{m}$ )	Smallest $\phi$ ( $\mu\text{m}$ )	Particle Count	Std Deviation $\phi$ ( $\mu\text{m}$ )
1	4.31	3.81	8.87	4.41	10.48	1.61	130	2.01
2	4.92	4.60	9.32	4.96	10.96	1.64	103	2.11
3	4.67	4.21	8.84	5.59	10.44	1.61	111	1.95
4	4.85	4.32	8.39	3.62	10.06	1.67	114	1.86
5	4.65	4.44	9.45	5.85	11.12	1.67	108	2.06
6	4.78	4.50	9.18	7.30	10.79	1.61	111	2.08
7	4.53	4.17	9.62	3.09	11.22	1.61	107	2.14
8	4.86	4.46	7.93	4.46	9.88	1.94	113	1.99
9	5.08	5.06	8.24	6.91	9.88	1.64	99	2.03
10	4.76	4.49	8.86	6.44	10.46	1.61	113	2.01

By inspecting the statistical data in Table 1, the good reproducibility of the photomicroscopy technique is confirmed. The average of the ten means is 4.74  $\mu\text{m}$ , and the average of all raw data is 4.73  $\mu\text{m}$ . Run 10 presents a mean value (4.76  $\mu\text{m}$ ) close to these. Run 1 has the farthest mean value (4.31  $\mu\text{m}$ ). The smallest detectable equivalent diameter for this configuration appears to be 1.61  $\mu\text{m}$ .

## 5.2 Laser Diffraction Analysis

Before presenting the analysis data, PSD diagrams are shown in Fig. 10. It was preferred because the simple data summarized in a table could give a misleading first impression.

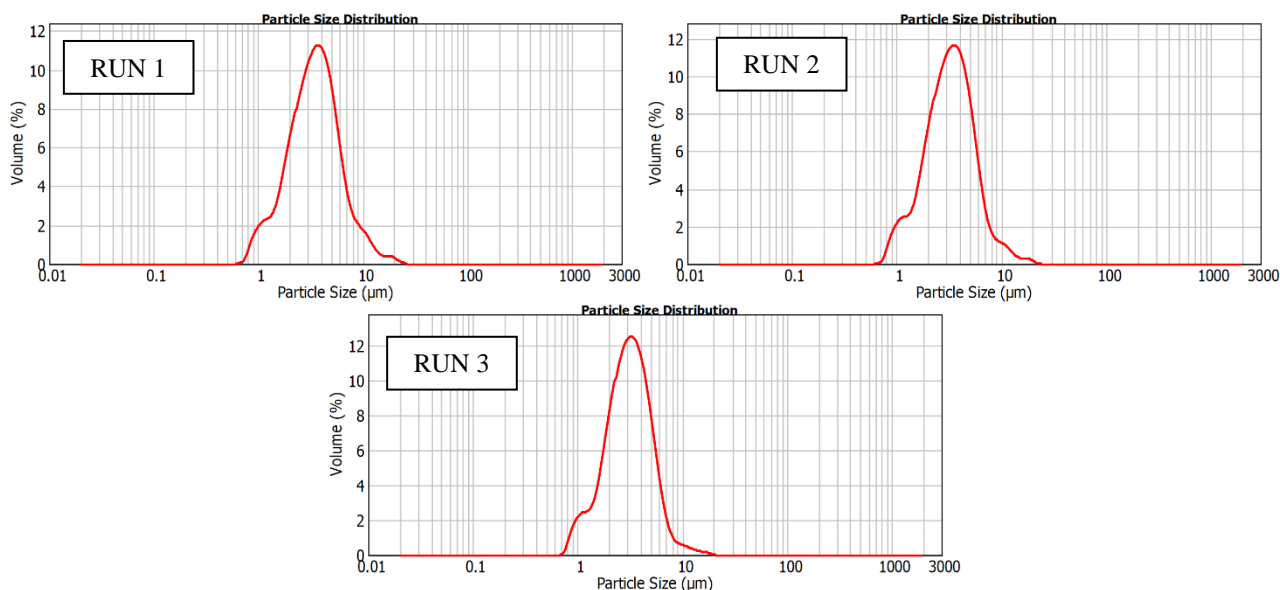


Figure 10. PSD diagram for laser diffraction analysis.

PSD diagrams in Fig. 10 are exactly the ones reported by Mastersizer Software. The similarities between them indicate a very good reproducibility. For investigations with Mastersizer, a “run” corresponds a set of analysis that reports averaged values. It must meet some criteria to be defined as a good analysis.

As stated in the user manual (Malvern, 2007a), “obscuration” is a measure of the amount of laser light lost due to the introduction of the sample into the analyzer beam. Acceptable value is 3 to 20% (ideal 10 to 20%). Photomicroscopy indicated that a good concentration of the solution should be 0.100 g/L, but the obscurity in the Mastersizer was a little over 20%. Thus, the solution concentration was adjusted to 0.080 g/L. This value was also used in photomicroscopy analysis.

Another important parameter is the “residual”, which is an indication of how well the calculated data was fitted to the measurement data (Malvern, 2007a). A good fit is indicated by a residual of under 1%. The solution in the beaker needs to be pumped to the optical drive to allow analysis. Three measurements would be made with the same solution, but calcium carbonate was scaling in the system (not surprising in the oil industry!). Thus, for each run, a new solution had to be prepared and the entire system washed. Table 2 summarizes the main parameters for laser diffraction analysis.

Table 2. Parameters for laser diffraction analysis.

Run	Obscuration (%)	Residual (%)	D(0.1) (μm)	D(0.5) (μm)	D(0.9) (μm)	Mean (μm)
1	17.5	0.645	1.597	3.451	6.921	4.07
2	19.3	0.808	1.538	3.241	6.107	3.73
3	15.3	1.497	1.547	3.069	5.491	3.42

Even reaching a “residual” of over 1% for Run 3, the result was found to be acceptable and was maintained, especially when analyzing the shape of PSD diagrams.

## 5.3 Comparison of the Techniques

Comparing the results of Tables 1 and 2, there is a tendency for higher average values in the photomicroscopy technique than in the laser diffraction technique. This is correct considering the high median values in Table 1 and the low D(0.5) values in Table 2. This is because the photomicroscopy set up used cannot measure particles smaller than 1.6 μm, which will be visually clear when overlapping diagrams are presented later.

It is important to keep in mind that the objective of this research is to verify if the photomicroscopy technique is able to estimate the particle size in solution without taking a sample. Choosing Run 2 diagram (Fig. 10) to graphically comparing the results of the two techniques, all the ten PSD diagrams for photomicroscopy runs are shown in Figure 11.

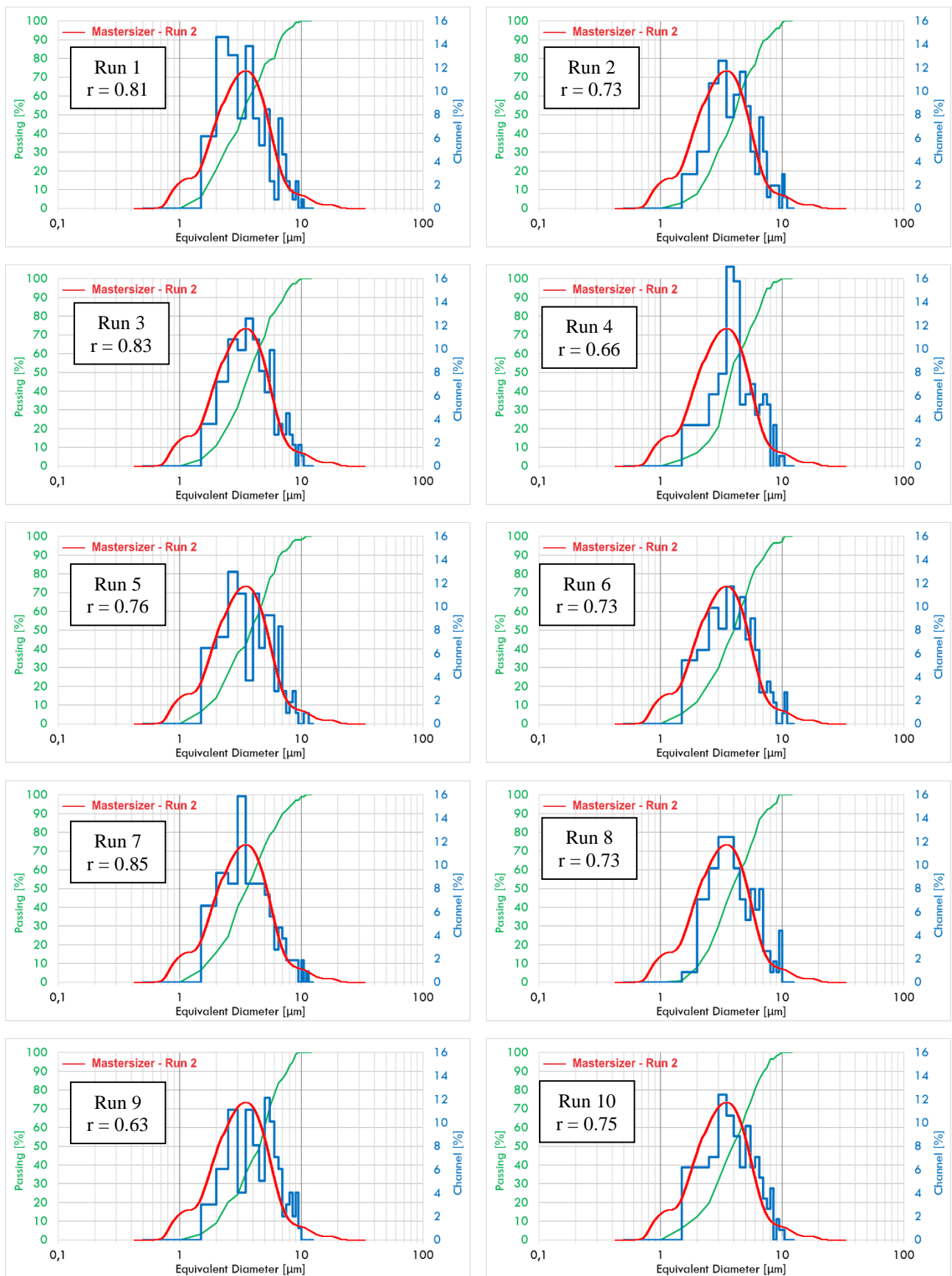


Figure 11. Comparative PSD diagrams. The red line represents laser diffraction while the blue line represents photomicroscopy technique.

Photomicroscopy diagrams also do not have the right tail, which corresponds for particles larger than 11  $\mu\text{m}$ . All photomicroscopy experiments were performed without stirring, while Mastersizer automatically shakes the solution when pumping an aliquot to the optical bench. Brownian motion cannot overcome gravitational forces for large particles such as larger than 11  $\mu\text{m}$ , so sedimentation is expected for an unstirred experiment.

Although photomicroscopy diagrams do not show the left and right tails, the weight of a high amount of particles below 1.6  $\mu\text{m}$  is greater than the weight of a low amount of particles above 11  $\mu\text{m}$ . This is correct considering  $D(0.1)$  always less than 1.6  $\mu\text{m}$  and  $D(0.9)$  never greater than 7  $\mu\text{m}$  (Table 2). This explains the fact that the photomicroscopy runs means are higher than the laser diffraction runs means.

Pearson correlation is a number ( $r$ ) between  $-1$  and  $+1$  that indicates how closely two data sets are related. In the case of  $r = +1$ , it indicates that there is a good direct correlation. For  $r = -1$ , the correlation is also good, but inverse. And for  $r = 0$ , there is no correlation. These  $r$ -values are reported in each run in Figure 11, which confirms a good correlation.

## 6. CONCLUSIONS AND COMMENTS

Although the two techniques are quite different in the way particles are detected and measured, the results presented here are relatively well similar. If a perfect correlation cannot be statistically observed to ensure that the photomicroscopy technique could replace laser diffraction or another proven technique for accurate particle size determination, the results reported here are excellent for the purpose of the research as a whole (see next section).

The shape of the diagrams in Figure 11 and the respective  $r$ -values indicate that photomicroscopy technique is able to determine the order of magnitude of particles in a solution above 1.6  $\mu\text{m}$ . By replacing the Mitutoyo 10X objective lens (34 mm focal length) with a 20X (20 mm) or 50X (13 mm) could capture particles as small as 0.5  $\mu\text{m}$ , but it is not possible considering the purpose of the main research (see next section).

## 7. OUTLOOK

The main objective of the research project is related to water-formed scale deposits under conditions that simulate the petroleum environment. That is, under pressure, temperature and subject to the presence of oil, gas, high salinity and other complicating factors for analysis under ambient conditions. To evaluate some phenomena under these situations, either there is no technique or it is too expensive or too dangerous. Thus, photomicroscopy technique can overcome some of these issues.

Associated with the photomicroscopy system, a pressurized reactor is being built with the availability of three viewing windows. The larger viewing window has a free diameter of 56 mm and a thickness of 29 mm. The other two have a free diameter of 35.5 mm and a thickness of 20 mm. With this arrangement, it is possible to operate under 100 bar pressure and 150  $^{\circ}\text{C}$  temperature. Thus, the focal length must be higher than 20 mm, which meets to the Mitutoyo 10X objective lens.

The experiments reported here were done with a 12 mm thick "viewing window" (Figs. 8 and 9). Other tests with 24 mm thickness brought the same results, without any loss of quality or information. It was enough to start the manufacturing process.

## 8. ACKNOWLEDGEMENTS

The authors would like to thank PETROBRAS, Brazil, to financially support this research study. The authors would like to thank LaPAQui team from CEUNES/UFES for their support in laser diffraction analysis.

## 9. REFERENCES

- Beck, R., and Andreassen, J.P., 2010, "The onset of spherulitic growth in crystallization of calcium carbonate," *Journal of Crystal Growth*, 312, p. 2226-2238.
- Brečević, L., and Nielsen, A.E., 1989, "Solubility of amorphous calcium carbonate," *Journal of Crystal Growth*, v. 98, p. 504-510. Amsterdam: Elsevier Science Publishers B. V.
- Brown, L., 2009, "Imaging Particle Analysis: Resolution and Sampling Considerations," Fluid Imaging Technologies, Inc.
- Cosmo, R.P., Pereira, F.A.R., Ribeiro, D.C., Barros, W.Q., and Martins, A.L., 2019, "Estimating CO<sub>2</sub> degassing effect on CaCO<sub>3</sub> precipitation under oil well conditions," *J. of Petroleum Sc. and Eng.*, 181, 106207.
- Cowan, J.C., and Weintritt, D.J., 1976, "Water-formed scale deposits," Houston, TX: Gulf Publishing Company.

- Crabtree, M., Eslinger, D., Fletcher, P., Miller, M., Johnson, A., and King, G., 1999, "Fighting scale-removal and prevention," *Oilfield Review*, p. 30-45, Autumn.
- Eseosa, A., and Atubokiki, A.J., 2011, "Prediction and monitoring of oilfield carbonate scales using Scale Check®," Society of Petroleum Engineers, SPE 150797, Nigeria Annual International Conference and Exhibition.
- Hennock, M., Rahalkar, R.R., and Richmond, P., 1984, "Effect of xanthan gum upon the rheology and stability of oil-water emulsions," 1274, *Journal of Food Science*, v. 49.
- Horiba, 2009, "The LA-950 laser diffraction technique," Technical Note, TN159, Horiba Instruments, Inc.
- Horiba, 2017, "A Guidebook for Particle Size Analysis," Horiba Instruments, Inc.
- Ingham, J.P., 2012, "Geomaterials Under the Microscope," Academic Press, ISBN 978-0-12-407230-5.
- ISO, 2009, "Particle Size Analysis – Laser Diffraction Methods," ISO 13320:2009, International Organization for Standardization.
- Kogo, M., Umegaki, and T., Kojima, Y., 2019, "Effect of pH on formation of single-phase vaterite," *Journal of Crystal Growth* 517, 35–38.
- Malvern, 2007a, "Mastersizer 2000 User Manual," MAN0384 Issue 1.0 March 2007 ADD0070-2.0 10/03/2010, Malvern Instruments Ltd.
- Malvern, 2007b, "Hydro 2000MU User Manual," MAN0387 Issue 1.0 April 2007, Malvern Instruments Ltd.
- MIS, 2019, "PAX-cam PAX-it™ Operational Manual," Manual Version: 0219, Midwest Information System, Inc.
- Pepper, I.L., Gerba, C.P., and Gentry, T.J., 2015, "Environmental Microbiology," Academic Press, ISBN 978-0-12-394626-3.
- Russell, D., Cleary, K., and Reeves, R., 2012, "Cryogenic probe station for on-wafer characterization of electrical devices," *American Institute of Physics, Review of Scientific Instruments* 83, 044703.
- Tai, C.Y., and Chen, P.-C., 1998, "Polymorphism of CaCO<sub>3</sub> precipitated in a constant-composition environment. *AIChE Journal*, Vol. 44, No. 8, p. 1790-1798.
- Tracy, S.L.; François, C.J.P.; and Jennings, H.M. The growth of calcite spherulites from solution - I. Experimental design techniques. *Journal of Crystal Growth*, v. 193, p. 374-381. Elsevier Science B.V., 1998.
- Waly, T.K.A., 2011, "Minimizing the use of chemicals to control scaling in SWRO: Improved prediction of the scaling potential of calcium carbonate," Taylor & Francis Group, LLC.
- Zhang, P., Allan, K., Hugh, and B., 2015, "Selection of Calcium Carbonate Scale Critical Values for Deepwater Production," In: SPE 173747-MS, Society of Petroleum Engineers. SPE International Symposium on Oilfield Chemistry.

## 10. RESPONSIBILITY NOTICE

The authors are the only responsible for the printed material included in this paper.